Catalysis Today 175 (2011) 299–309

Contents lists available at ScienceDirect

Catalysis Today

journal homepage: www.elsevier.com/locate/cattod

Enhanced catalytic activity of Fe bimetallic modified PAN fiber complexes prepared with different assisted metal ions for degradation of organic dye

Yongchun Dong[a,b,*], Zhenbang Han[a,b], Siming Dong[c], Jinna Wu[a], Zhizhong Ding[a]

[a] Division of Textile Chemistry & Ecology, School of Textiles, Tianjin Polytechnic University, Tianjin 300160, China
[b] State Key Laboratory Breeding Base of Photocatalysis, Fuzhou University, Fuzhou 350002, China
[c] Department of Materials Science and Engineering, Tsinghua University, Beijing 100085, China

ARTICLE INFO

Article history:
Received 30 October 2010
Received in revised form 15 February 2011
Accepted 12 April 2011
Available online 11 May 2011

Keywords:
PAN fiber
Metal ions
Bimetallic complex
Fenton catalyst
Dye degradation

ABSTRACT

Two transition metal ions (Cu^{2+} and Co^{2+}) and two rare earth metal ions (Ce^{3+} and La^{3+}) were used as the assisted metal ions, respectively to prepare the transition metal and rare metal assisted Fe bimetallic amidoximated polyacrylonitrile (AO-PAN) fiber complexes. And their coordination configuration and visible light adsorption properties were examined by coordination number determination and UV–vis–DRS. Then the catalytic performance of these complexes was evaluated as the heterogeneous Fenton catalysts in Rhodamine B degradation by changing the nature and dosage of the assisted ions added. The results indicated that the incorporation of the assisted metal ions led to Fe bimetallic AO-PAN complexes with the more unsaturated configurations than Fe monometallic AO-PAN complex due to the changes in their coordination numbers. The visible light adsorption properties of Cu–Fe or Ce–Fe AO-PAN bimetallic complexes varied significantly with their Cu/Fe or Ce/Fe molar ratio. Fe bimetallic AO-PAN complex showed a higher catalytic performance as the Fenton catalysts toward the dye degradation than Fe monometallic AO-PAN complex. And the nature and dosage of the assisted metal ions can affect their catalytic activities. Ce–Fe bimetallic AO-PAN complex was found to have a better stability in a wider pH range than Cu–Fe bimetallic AO-PAN complex.

1. Introduction

In recent years, active heterogeneous Fenton catalysis is increasingly replacing the homogeneous system with drawbacks of pH limitation and catalyst regeneration in catalysis research [1,2]. And several heterogeneous Fenton processes for decomposing organic pollutants have been described, in which zeolite [3], Nafion membrane [4], alginate microcapsules [5] and the modified Polyacrylonitrile (PAN) fiber [6,7] were employed to immobilize Fe^{3+} ions. However, the deactivation of Fe^{3+} ions after being immobilized on the materials was often observed in the heterogeneous Fenton process. To achieve the desirable catalytic activity, the supported Fe catalysts are often modified by adding certain metal ions. For example, other transition metal ions especially Cu^{2+} ions are introduced to help the Fe-containing catalysts improving catalytic performance. Guimaraes et al. [8] found that doping the Cu^{2+} ions into the goethite led to a strong increase in the catalytic activity of Cu–Fe bimetallic heterogeneous Fenton catalyst during the quinoline oxidation. Fan et al. [9] reported that the Fe and Cu salen complexes simultaneously encapsulated in zeolite Y showed much higher activity than the Cu (salen)Y and Fe (salen)Y or their physical mixtures in the oxidation of cyclohexane. On the other hand, the rare earth metal ions including Ce ions and La ions were also used as the powerful modifying agents for catalysts because the coordination of these ions in the materials can affect the catalytic properties by their excellent optical and redox properties [10,11]. Zhang et al. [12] showed that the Ce doped Fe oxide demonstrated much better decolorization performance for the azo dye than the single Fe system. Carriazo et al. [13] pointed out that the addition of Ce into the Fe-containing bentonite showed favorable results in the catalytic activity when dealing with the elimination of phenol. It is generally believed that the assisted metals could generate the synergetic effect in the catalyst, allowing the increase of metallic dispersion properties and favoring the redox properties of the active metallic phase.

The modified PAN fibrous complex is regarded as an attractive catalytic material with unique advantages including lower cost, suitable chemical and mechanical stability as well as easy separation of the catalyst after the reaction [6,14]. This is because PAN fiber can be easily introduced into various functional groups through the transformation of its nitrile groups, which makes it effective as a heterogeneous catalyst support to immobilize metal ions by coordi-

* Corresponding author at: Division of Textile Chemistry and Ecology, School of Textiles, Tianjin Polytechnic University, 63 Chenglin Road, Hedong District, Tianjin 300160, P.R. China, Tel.: +86 22 24528430, fax: +86 22 24528054.
E-mail address: dyefib@yahoo.com.cn (Y. Dong).

0920-5861/$ – see front matter © 2011 Elsevier B.V. All rights reserved.
doi:10.1016/j.cattod.2011.04.026

nation bonds. Ishtchenko et al. [6,7] have prepared a heterogeneous Fenton catalyst by ligating the Fe ions onto the surface of the modified PAN fiber with a mixture of hydrazine and hydroxylamine for the decomposition of real effluent from dyeing processes. Our recent study [15] found that the amidoximated PAN fiber could also coordinate with Fe^{3+} ions to prepare the heterogeneous Fenton catalyst for the dye degradation. However, there has been no report on the addition of the transition metal and rare earth metal ions as the assisted ions to improve the catalytic performance of Fe amidoximated PAN fiber complexes for the treatment of organic pollutants. In this study, two transition metal ions (Cu^{2+} and Co^{2+}) and two rare earth metal ions (Ce^{3+} and La^{3+}) were selected as the assisted metal ions to prepared different Fe bimetallic amidoximated PAN fiber complexes. The present work is purposed to evaluate and compare the incorporation of the transition metal and rare earth metal ions as the assisted ions on the coordination structure and light adsorption property of the Fe amidoximated PAN fiber complexes because these features can significantly effect their catalytic properties. Then the catalytic performance of these resulting bimetallic amidoximated PAN fiber complexes were assessed and compared in the degradation of Rhodamine B (RhB) with H_2O_2 by changing the nature and dosage of the assisted ion. Finally, a typical Fe–Cu bimetallic amidoximated PAN fiber complex was used to investigate the influence of Cu^{2+} ions as the assisted metal ions in the complex on the H_2O_2 decomposition and active radical generation during the dye degradation using UV–vis spectroscopy, COD measurement and DMPO-trapping ESR technique.

2. Experimental

2.1. Materials and chemicals

PAN knitting bulky yarns (abbreviations PAN yarn) consisted of twisted PAN fibers (the content of acrylonitrile: 86.96%) were commercial available. $NH_2OH{\cdot}HCl$ and H_2O_2 (30%, w/w) were of analytical grade. $FeCl_3{\cdot}7H_2O$, $CuSO_4{\cdot}5H_2O$, $CoSO_4{\cdot}7H_2O$, $CeCl_3{\cdot}7H_2O$ and $LaCl_3{\cdot}7H_2O$ were used as the metal ions sources, respectively. 5,5-Dimethyl-l-pyroline-N-oxide (DMPO), horseradish peroxidase (POD), *N*,*N*-diethyl-*p*-phenylene-deamine (DPD) and Rhodamine B were of laboratory agent grade and used without further purification. Double distilled and deionized water was used throughout the study.

2.2. Preparation of metallic modified PAN fiber complexes

2.2.1. Amidoximation of PAN yarns

The amidoximation of PAN yarns was carried out using a method reported in our previous study [15]. Dried PAN yarns were added into a solution containing the appropriate concentrations of $NH_2OH{\cdot}HCl$ and NaOH in a flask with a thermometer and agitator. The mixed solution was heated for 2 h with stirring at 68 °C to accomplish the amidoximation. Then the obtained amidoximated PAN yarns (denoted as AO-PAN) were repeatedly washed with distilled water until washings were neutral and dried under vacuum. The degree of conversion from nitrile group to amidoxime group of AO-PAN was calculated to be 60.09%. The amidoximation of PAN fiber was described by Eq. (1).

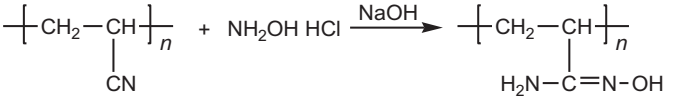

(1)

2.2.2. Fe monometallic AO-PAN complex

Five grams of AO-PAN were immersed in 150 mL of coordination solution containing 0.10 mol L^{-1} $FeCl_3$ and then the mixture was treated at 50 °C and pH 2.0–3.0 for a given time under continuous agitation. The obtained Fe monometallic AO-PAN complex (denoted as Fe-AO-PAN) was filtered and washed with deionized water, and then dried under vacuum at 60 °C for 4 h. The residual concentration of Fe^{3+} ions in solution after coordination was determined using a WXF120 atomic absorption spectrometry (AAS, Beijing Rayleigh Analytical Instrument Corp.) for calculating the Fe content ($C_{Fe\text{-}PAN}$) of the complex.

2.2.3. Transition metal assisted Fe metallic AO-PAN complexes

These complexes were synthesized similarly to Fe-AO-PAN by using the mixed coordination solutions containing different concentrations of Fe^{3+} and Cu^{2+} or Co^{2+} ions during the coordination processes. Fe–Cu and Fe–Co bimetallic AO-PAN complexes (denoted as Fe–Cu-AO-PAN and Fe–Co-AO-PAN) with different molar ratios of Fe to Cu or Co ion (abbr. Cu/Fe or Co/Fe molar ratio) were synthesized by adjusting the concentrations of the metal ions in coordination solution, and in which the concentrations of total metal ions were kept constant at 0.10 mol L^{-1}. The Cu content ($C_{Cu\text{-}PAN}$) or the Co content ($C_{Co\text{-}PAN}$) in these complexes was also measured using AAS method mentioned above.

2.2.4. Rare earth metal assisted Fe bimetallic AO-PAN complexes

These complexes were prepared similarly to those transition metals assisted Fe bimetallic AO-PAN complexes by mixing $FeCl_3$ with $CeCl_3$ or $LaCl_3$ in the coordination solution, respectively. And the final complexes were also denoted as Fe–Ce-AO-PAN and Fe–La-AO-PAN, correspondingly. Their Ce content ($C_{Ce\text{-}PAN}$) and La content ($C_{La\text{-}PAN}$) were measured and calculating by determining the residual rare metal ions in solution after coordination by a Na_2-EDTA-based titrimetric method.

2.3. Determination of coordination number

To measure the coordination numbers of AO-PAN Fe metallic complexes, several reaction systems with different molar ratios of the concentration of amidoxime groups on AO-PAN to the initial concentration of the metal ions in coordination solution (denoted as $[AO\text{-}PAN]/[M^{n+}]_0$) were established by immersing various weight of AO-PAN into 150 mL coordination solution containing metal ions or their mixture. The coordination reactions in these systems were conducted at 50 °C until the reaction equilibrium was reached. Then the equilibrium concentrations of the metal ions in solution (denoted as $[M^{n+}]_e$) were measured using the same method as above and plotted as a function of the corresponding $[AO\text{-}PAN]/[M^{n+}]_0$, finally the coordination numbers for these complexes were determined by using the tangent method.

2.4. Light adsorption measurement

The light adsorption properties of these prepared samples were evaluated by measuring their diffuse reflectance UV–vis spectra (UV–vis–DRS), which were recorded on a Varian Cary 500 UV–vis–NIR spectrometer (Varian Inc., USA) in the 200–800 nm range with $BaSO_4$ as the reflectance standard.

2.5. Catalytic study

The metallic AO-PAN complexes were assessed as the Fenton catalysts in the RhB degradation performed in a specially designed photoreaction system, the diagram of which was present in Fig. 1. A cut-off filter was used to ensure a complete visible light irradiation

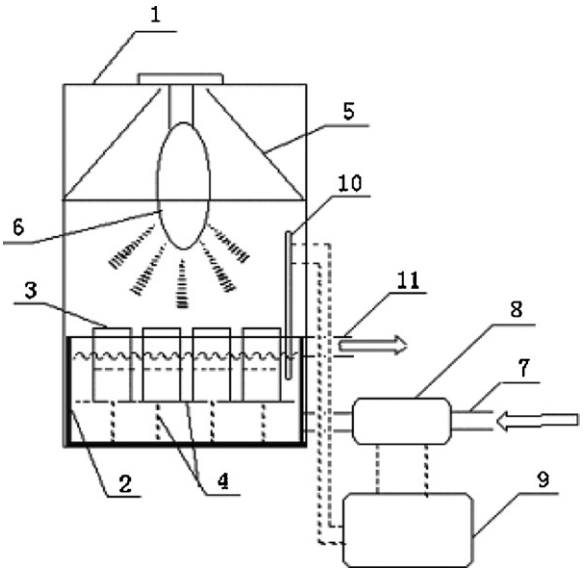

Fig. 1. The schematic diagram of photoreaction system. 1. chamber, 2. water bath, 3. glass vessel, 4. support, 5. lamp-chimney, 6. mercury lamp, 7. water in, 8. electromagnetic valve, 9. relay, 10. thermometer, 11. water out.

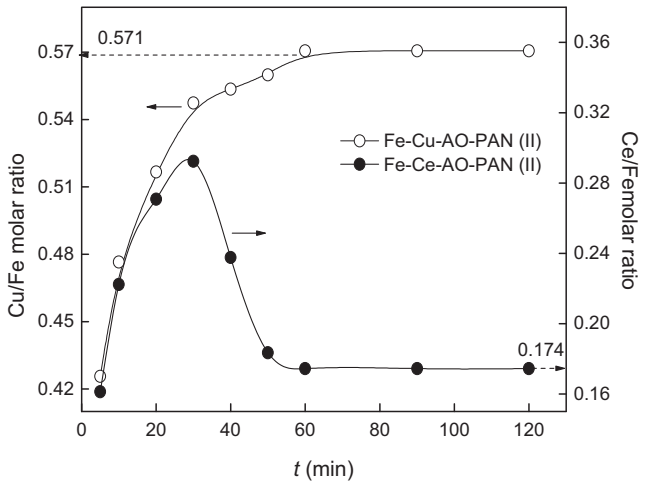

Fig. 2. Obvious changes in Cu/Fe and Ce/Fe molar ratios during the reaction processes.

($\lambda > 420$ nm). Light intensity inside photoreaction system was measured to be 9.11 mW cm^{-2} using FZ-A radiometer (BNU Light and Electronic Instrumental Co., China), and the temperature in reaction vessel was kept at 25 ± 1 °C. Unless noted otherwise, all the photodegradation experiments were carried out in 100 mL of test solution containing 0.02 mmol L^{-1} RhB and 3.0 mmol L^{-1} H_2O_2 at an initial pH of 6.0, with 0.50 g of the metallic AO-PAN complexes. At given time intervals, 1–2 mL of the test solution was withdrawn from the reaction vessel and analyzed on a UV-2401 Shimadzu spectrophotometer (Shimadzu Co. Japan). The decoloration percentage of the dye was expressed as: $D\% = (1 - C/C_0) \times 100\%$, where C_0 and C are the initial concentration and the residual concentration of the dye (mmol L^{-1}), respectively. The UV–vis spectrum from 190 to 800 nm was also recorded. The COD analysis were performed by the dichromate method according to the Chinese National Standard GB 11914-89 based on ISO/DIS 6060, and the COD removal percentage of the dye was calculated as follows: COD removal $\% = (1 - \mathrm{COD_t}/\mathrm{COD_0}) \times 100\%$, where $\mathrm{COD_0}$ and $\mathrm{COD_t}$ are the COD values (mg L^{-1}) at reaction times 0 and t, respectively. H_2O_2 concentration in the solution during the dye degradation was determined through the spectrophotometric DPD method with POD-catalyzed oxidation product of DPD analyzed at 551 nm [16]. ESR signals of the radical spin-trapped by DMPO were examined on a Bruker ESP 300E spectrometer with an irradiation source of Quanta-Ray Nd: YAG pulsed laser system ($\lambda = 532$ nm), and the same quartz capillary tube is used throughout the ESR measurements to minimize the experimental errors. Cyclic voltammetric measurement of Fe metallic AO-PAN complexes was performed on a LK3100 electrochemical workstation (Tianjin Lanlike Co., China).

3. Results and discussion

3.1. Preparation of metallic AO-PAN complexes

Simultaneous coordination of Fe^{3+} and Cu^{2+}or Ce^{3+} ions as an assisted metal ion with AO-PAN was conducted by controlling the initial concentrations of two metal ions in aqueous solution ($[Fe^{3+}]_0$ and $[Cu^{2+}]_0$ or $[Ce^{3+}]_0$) and reaction duration using the methods mentioned above to obtain two series of the Fe bimetallic AO-PAN complexes with similar total metal contents (C_{tol}). And both Cu/Fe and Ce/Fe molar ratios were calculated and presented in Tables 1 and 2.

It is obvious from the data listed in Tables 1 and 2 that Cu/Fe or Ce/Fe molar ratios of these complexes were greatly affected by both nature and concentration of the metal ions in coordination solution. In the case of Fe–Cu bimetallic AO-PAN complexes, their Cu/Fe molar ratios increase as the $[Cu^{2+}]_0$ increasing. However, it should be stated that when Cu^{2+} ions have the same initial concentration (0.05 mol L^{-1}) as Fe^{3+} ions, the Cu/Fe molar ratio of Fe–Cu-AO-PAN(II) is 0.571, much less than 1.00, suggesting that AO-PAN has much higher affinity for Fe^{3+} ions than Cu^{2+} ions at the same conditions. The main reason is that AO-PAN prefers to react with Fe^{3+} ions as the hard acid to form a stable complex, because it has amino and hydroxyl groups, thus showed the structural characteristics of hard base [17]. Additionally, the stronger polarity of Fe^{3+} ions [6] and the lower ligand field stabilization energy (LFSE) of the octahedral Fe^{3+} complexes [17,18] were also responsible for the higher complex ability of Fe^{3+} ions to AO-PAN. It is seen from Table 2 that Fe–Ce bimetallic AO-PAN complexes exhibit the similar Ce/Fe molar ratio variation to the Cu/Fe molar ratio. When $[Ce^{3+}]_0$ is equal to $[Fe^{3+}]_0$, the Ce/Fe molar ratio of Fe–Ce-AO-PAN(II) is 0.174, much lower than Cu/Fe molar ratio of Fe–Cu-AO-PAN(II). To further understand the difference in coordination behavior between transition and rare earth metal ions as the assisted metal ions with AO-PAN in the presence of Fe^{3+} ions, Fe–Cu-AO-PAN(II) and Fe–Ce-AO-PAN(II) were synthesized, respectively. And their Cu/Fe or Ce/Fe molar ratio was calculated during the preparation processes, and shown in Fig. 2.

Fig. 2 shows that Cu/Fe molar ratio increased significantly within about 30 min, indicating that much less Cu^{2+} ions than Fe^{3+} ions had coordinated with AO-PAN in the beginning of reaction process. And then Cu/Fe molar ratio increased gradually and was kept to be 0.571 at the end of reaction. This confirms that the coordination equilibrium between two metal ions and AO-PAN was obtained during the reaction time of 120 min. On the other hand, Ce/Fe molar ratio presented the similar change to Cu/Fe molar ratio and increased up to a point within about 30 min. Over this point, Ce/Fe molar ratio dropped off rapidly with the prolongation of reaction time. A constant Ce/Fe molar ratio was 0.174 when the coordination of two metal ions with AO-PAN reached equilibrium. Furthermore, Fe–Co-AO-PAN(II) and Fe–La-AO-PAN(II) were also prepared when Co^{2+} or La^{3+} and Fe^{3+} ions have an equal initial concentration (0.05 mol L^{-1}) to compare the coordination property of four assisted metal ions with AO-PAN in the presence of Fe^{3+} ions, and the molar ratios of Fe to different assisted metal are ranked

Table 1
Fe–Cu bimetallic AO-PAN complexes with different Cu/Fe molar ratios.

Designation of samples in solution (mol L^{-1})	Conc. of metal ions		Metal contents in the complexes (mmol g^{-1})			Cu/Fe molar ratio
	$[Fe^{3+}]_0$	$[Cu^{2+}]_0$	$C_{Fe\text{-}PAN}$	$C_{Cu\text{-}PAN}$	C_{tol}	
Fe-AO-PAN	0.10	0.00	2.519	0.000	2.519	0.000
Fe–Cu-AO-PAN(I)	0.075	0.025	2.016	0.388	2.404	0.193
Fe–Cu-AO-PAN(II)	0.05	0.05	1.544	0.881	2.425	0.571
Fe–Cu-AO-PAN(III)	0.025	0.075	1.095	1.211	2.306	1.106
Cu-AO-PAN	0.00	0.10	0.000	2.387	2.387	–

Table 2
Fe–Ce bimetallic AO-PAN complexes with different Ce/Fe molar ratios.

Designation of samples in solution (mol L^{-1})	Conc. of metal ions		Metal contents in the complexes (mmol g^{-1})			Ce/Fe molar ratio
	$[Fe^{3+}]_0$	$[Ce^{3+}]_0$	$C_{Fe\text{-}PAN}$	$C_{Ce\text{-}PAN}$	C_{tol}	
Fe-AO-PAN	0.10	0.00	2.519	0.000	2.519	0.000
Fe–Ce-AO-PAN(I)	0.075	0.025	2.349	0.073	2.422	0.031
Fe–Ce-AO-PAN(II)	0.05	0.05	2.087	0.363	2.450	0.174
Fe–Ce-AO-PAN(III)	0.025	0.075	1.801	0.581	2.382	0.323
Ce-AO-PAN	0.00	0.10	0.000	2.375	2.375	–

in this order: Cu/Fe > Co/Fe > Ce/Fe > La/Fe at the same condition. The results suggest that two rare earth metal ions could coordinate with AO-PAN with more difficulty than transition metal ions in the presence of Fe^{3+} ions. This is because the 4f electrons of rare earth metal ions are in the inner orbital of the atomic structure, so that the ligand field has less effect on them and the rare earth metal ions have much lower LFSE values (4.18 kJ mol^{-1}) than d-transition metal ions (≥418 kJ mol^{-1}) [18]. Comparing two transition metal ions, Cu^{2+} ions show higher reactivity in the combined coordination with Fe^{3+} ions than Co^{2+} ions to form Fe bimetallic AO-PAN complex. The main reason is that the second ionization potential (IP) of Cu^{2+} ion is higher than that of Co^{2+} ion [19–21] and the Cu^{2+} complexes have higher stability than Co^{2+} complexes according to the Irving-Williams series [21]. Another reason is that the complex of Cu^{2+} ion with ligand should distort according to the John-Teller theorem [18]. On the other hand, La^{3+} ion has low ability to form AO-PAN complexes due to its bigger radius than Ce^{3+} ion as a consequence of the lanthanide contraction. Since lanthanides ions show a tendency to form complex and their stability increases with increasing atomic number and decreasing ionic radius [21,22].

Coordination number is generally defined as the number of ligands bonded to the central atom, which is an important characteristic of a coordination compound and in close relation to the molecular structure and properties. In this study, the coordination numbers for several monometallic AO-PAN complexes, especially Fe-AO-PAN, Cu-AO-PAN and Ce-AO-PAN, and Fe bimetallic AO-PAN complexes, especially Fe–Cu-AO-PAN(II) and Fe–Ce-AO-PAN(II) were measured through the variation curve of $[M^{n+}]_e$ with [AO-PAN]/$[M^{n+}]_0$ using tangent method and the results are presented in Figs. 3–5.

Fig. 3 shows that $[Fe^{3+}]_e$ decreased significantly with [AO-PAN]/$[Fe^{3+}]_0$ increasing, and no further reduction was observed after [AO-PAN]/$[Fe^{3+}]_0$ was above 6 in the absence or presence of Cu^{2+} or Ce^{3+} ions. This means the coordination between AO-PAN and Fe^{3+} ions in solution achieved equilibrium at the critical molar ratio. More importantly, a corresponding [AO-PAN]/$[Fe^{3+}]_0$ was obtained to be about 3 by the intersection between both tangents, indicating that one Fe^{3+} ion coordinated with three amidoxime groups from AO-PAN in the resulting Fe-AO-PAN. Thus Fe^{3+} ion as a central cation that had a coordination number of 6 in this complex. This was in agreement well with the result reported in our previous work [23]. Although $[Fe^{3+}]_e$ in the presence of Cu^{2+} or Ce^{3+} ions is slightly higher than that in the absence of Cu^{2+} or Ce^{3+} ions at the same [AO-PAN]/$[Fe^{3+}]_0$, the coordination number of Fe^{3+} ion in the resulting Fe–Cu-AO-PAN(II) or Fe–Ce-AO-PAN(II)

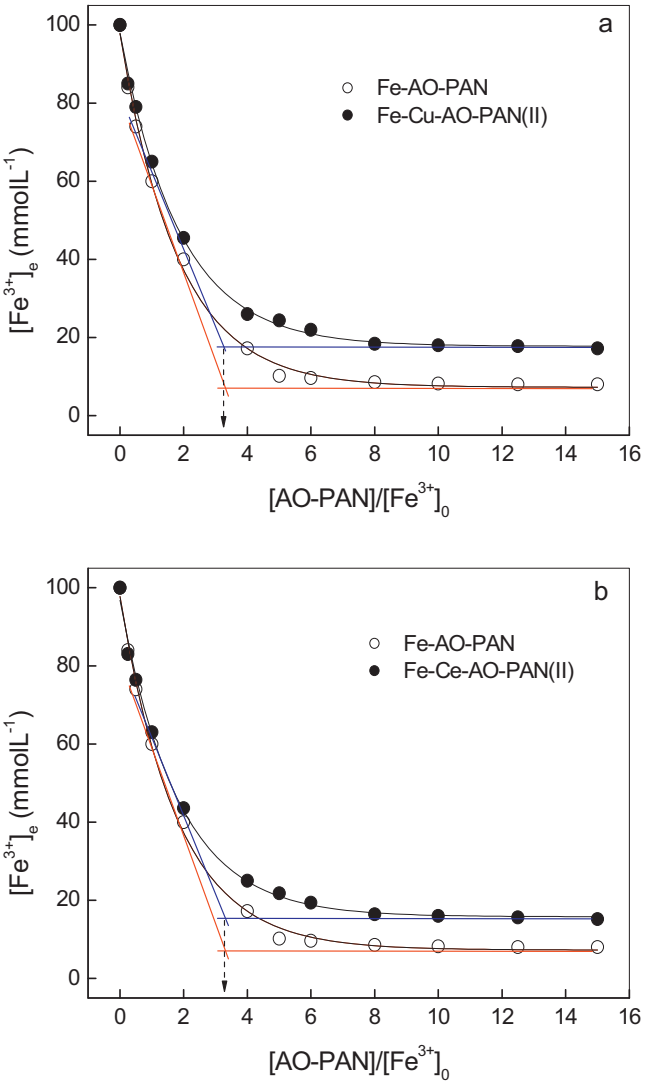

Fig. 3. Relationship between [AO-PAN]/$[Fe^{3+}]_0$ and $[Fe^{3+}]_e$.

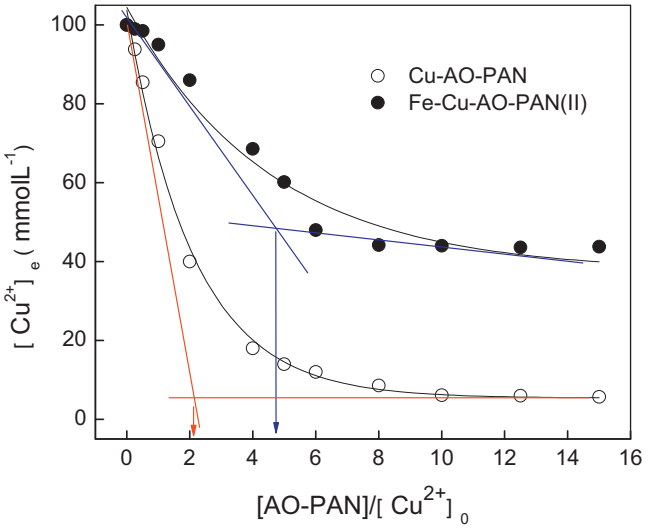

Fig. 4. Relationship between $[AO\text{-}PAN]/[Cu^{2+}]_0$ and $[Cu^{2+}]_e$.

was measured to be still 6. This proposed that the coordination behavior of Fe^{3+} ion with AO-PAN was hardly affected by the presence of Cu^{2+} or Ce^{3+} ions due to the higher affinity between Fe^{3+} ion and AO-PAN. On the other hand, the similar variations of $[Cu^{2+}]_e$ or $[Ce^{3+}]_e$ with $[AO\text{-}PAN]/[Cu^{2+}]_0$ or $[AO\text{-}PAN]/[Ce^{3+}]_0$ was also observed in Fig. 4 or Fig. 5. And the coordination number of Cu^{2+} or Ce^{3+} ion in the resulting Cu-AO-PAN or Ce-AO-PAN was also determined to be 4 or 10 in the absence of Fe^{3+} ions. However, $[Cu^{2+}]_e$ in the presence of Fe^{3+} ions was much higher than that in the absence of Fe^{3+} ions at the same $[AO\text{-}PAN]/[Cu^{2+}]_0$, and the difference between them remarkably increased as $[AO\text{-}PAN]/[Cu^{2+}]_0$ increasing, which led to an obvious change in the coordination number (10) of Cu^{2+} ion in Fe–Cu-AO-PAN(II). Also, an insignificant shift in the coordination number of Ce^{3+} ion in Fe–Ce-AO-PAN(II) had been also found in Fig. 5. Besides, the coordination numbers for another two Fe bimetallic AO-PAN complexes (Fe–Co-AO-PAN(II) and Fe–La-AO-PAN(II)) were also measured and compared with those for Co-AO-PAN and La-AO-PAN, respectively. And little difference in coordination number change between Fe–Co-AO-PAN(II) and Fe–Cu-AO-PAN(II) or Fe–La-AO-PAN(II) and Fe–Ce-AO-PAN(II) was observed. These results reveal that these Fe bimetallic AO-PAN complexes, particularly Fe–Cu-AO-PAN(II) are considerably

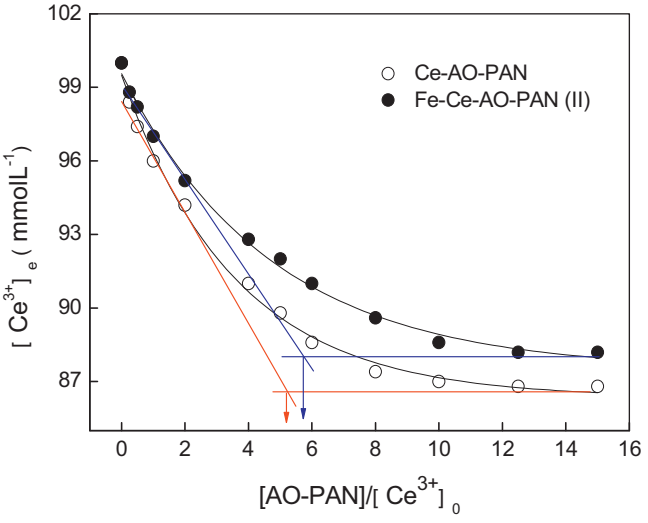

Fig. 5. Relationship between $[AO\text{-}PAN]/[Ce^{3+}]_0$ and $[Ce^{3+}]_e$.

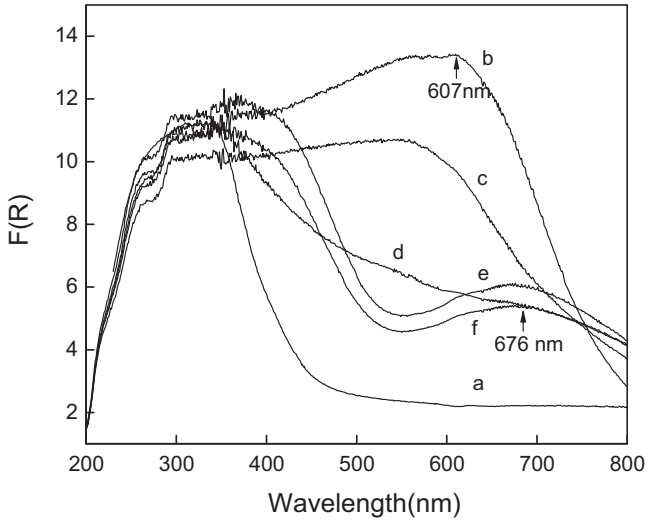

Fig. 6. Effect of Cu/Fe molar ratio on UV–vis–DR spectra of Fe–Cu bimetallic AO-PAN complexes: (a) AO-PAN, (b) Fe-AO-PAN, (c) Fe–Cu-AO-PAN(I), (d) Fe–Cu-AO-PAN(II), (e) Fe–Cu-AO-PAN(III) and (f) Cu-AO-PAN.

different from the monometallic AO-PAN complexes in terms of coordination configuration owing to the competition and interaction between Fe^{3+} and assisted metal ions for the amidoxime groups during the reaction processes, which may be responsible for their different catalytic characteristics.

3.2. Light adsorption properties of AO-PAN bimetallic complexes

The UV–vis–DRS is a suitable analytical technique to study solid substances, particularly complexes to obtain information on the coordination environment, oxidation state of the embedded transition and rare earth metal ions [24,25]. This is because different molecules absorb radiation of different wavelengths. An absorption spectrum will show a number of absorption bands corresponding to structural groups within the molecule. Therefore, this technique was used to evaluate the visible light adsorption properties of the metallic AO-PAN complexes and examine the interaction of Cu^{2+} or Ce^{3+} ions with Fe^{3+} ions in the microenvironment of the complexes in this study. Cu^{2+} and Ce^{3+} ions were chosen as the typical

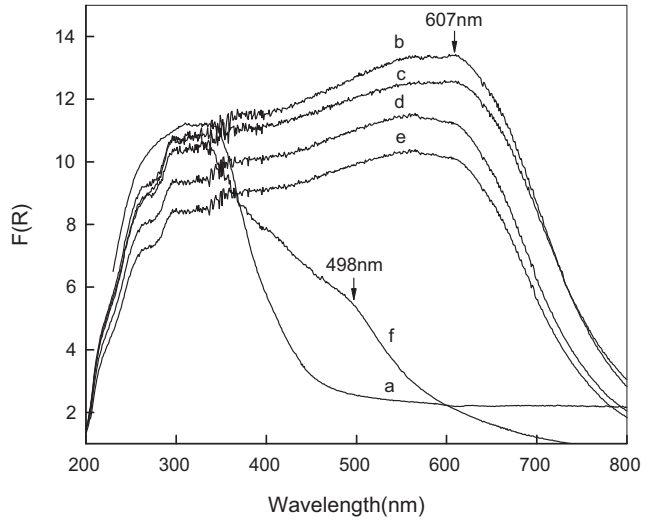

Fig. 7. Effect of Ce/Fe molar ratio on UV–vis–DR spectra of Fe–Ce bimetallic AO-PAN complexes: (a) AO-PAN, (b) Fe-AO-PAN, (c) Fe–Ce-AO-PAN(I), (d) Fe–Ce-AO-PAN(II), (e) Fe–Ce-AO-PAN(III) and (f) Ce-AO-PAN.

Table 3
k_d and k_r values in the presence of the catalysts with different assisted metal ions.

Catalysts		In the dark		Under visible irradiation	
		k_d (min^{-1})	R	k_r (min^{-1})	R
Fe-AO-PAN	C_{tol} = 2.52 mmol g^{-1} Cu/Fe = 0.57	0.0149	0.9965	0.0492	0.9948
Fe–Cu-AO-PAN	C_{tol} = 2.43 mmol g^{-1} Co/Fe = 0.56	0.0502	0.9993	0.0767	0.9992
Fe-Co-AO-PAN	C_{tol} = 2.41 mmol g^{-1} Ce/Fe = 0.17	0.0416	0.9997	0.0726	0.9964
Fe–Ce-AO-PAN	C_{tol} = 2.45 mmol g^{-1} La/Fe = 0.12	0.0513	0.9991	0.0967	0.9957
Fe-La-AO-PAN	C_{tol} = 2.40 mmol g^{-1}	0.0488	0.9996	0.0852	0.9934

transition and rare earth metal ions, respectively, because Co^{2+} and La^{3+} ions have the similar coordination tendency and configuration of their complexes with AO-PAN mentioned above. Figs. 6 and 7 presented the UV–vis–DRS of Fe–Cu and Fe–Ce bimetallic AO-PAN complexes.

Figs. 6 and 7 show that AO-PAN displays a characteristic broad band centered at 332 nm in the UV region due to its transitions of π electrons to the π^* excited state. It should be stressed that there is a significantly broad and strong absorption in the UV and visible region after coordination of AO-PAN with the metal ions, especially Fe^{3+} ion. While the absorption band in the visible region is attributed to the d–d transitions of the metal ions and the ligand-to-metal charge transfer (LMCT) transitions from AO-PAN toward metal ion in the complexes. It is known that the d-orbital symmetry of the metal ions may be broken by the coordination effect of the ligands and their forbidden d–d transition is allowed [26], thus often leading to the weak adsorption in the visible region. On the other hand, LMCT transitions can cause strong absorption in the visible region, especially for the O-donor ligand complexes since one oxygen atom could provide two lone pair electrons [27,28]. In the case of Fe–Cu bimetallic AO-PAN complexes, a broad and intense band centered at 607 nm in the spectrum of Fe-AO-PAN is mainly due to the LMCT transitions (O2p–Fe3d), which is in agreement with the LMCT bands of O-donor ligand with Fe^{3+} complexes being located between 500 and 700 nm [28]. The incorporation of Cu^{2+} ion in Fe-AO-PAN leads to a less intensive and narrower absorption of light in the visible region of the spectra. Moreover, there is an obvious peak at 676 nm in the visible region in the spectrum of Cu-AO-PAN, which is probably due to the d–d transition of Cu^{2+} ions, rather than the LMCT transitions (O2p–Cu3d) since Cu^{2+} ions have nearly complete 3d orbital [29]. Fe–Cu-AO-PAN(II) shows a uniquely different spectrum from those of the other Fe–Cu bimetallic AO-PAN complexes, and the characteristic bands from Fe-AO-PAN and Cu-AO-PAN are also observed in its UV–vis–DRS spectrum. This may be owing to a more dramatic interaction of Fe^{3+} with Cu^{2+} ions in Fe–Cu-AO-PAN(II) than the other two AO-PAN bimetallic complexes. In the case of Fe–Ce bimetallic AO-PAN complexes, the coordination of Ce^{3+} ions in the complexes caused a gradual decreased absorption of light in the visible region and the band centered at 607 nm in the spectrum of Fe-AO-PAN is found to shift to lower position with Ce/Fe molar ratio increasing. It is also seen from Fig. 7 that Ce-AO-PAN can absorb much less visible light, especially at higher position compared with Fe-AO-PAN. And a small shoulder observed at 498 nm is related to $O \rightarrow Ce^{3+}$ charge transfer transitions. The change in spectral features of the Fe–Ce bimetallic AO-PAN complexes indicates the presence of Ce^{3+} ion in a different chemical environment causes the varied band transition in the UV and visible region. It is summarized that the light adsorption feature of two Fe bimetallic AO-PAN complexes varied significantly with their Cu or Ce content. And the spectral features change dramatically when Cu ion is associated with Fe metallic AO-PAN complex. Comparing Fe–Cu-AO-PAN(II) and Fe–Ce-AO-PAN(II), it can be found that the latter exhibits much more intensive light adsorption, particular in the visible region than the former, possibly because Cu content in the former is much higher than Ce content in the latter. Besides, this is owing to a big difference in the chemical environments that Cu^{2+} or Ce^{3+} ion locates at. Consequently, it is believed that two Fe bimetallic AO-PAN complexes with low Cu/Fe or Ce/Fe molar ratio may be used as the effective photocatalysts and this assures the potential utilization of the visible light of solar irradiation because they are more activated throughout the UV and visible wavelengths where light absorption occurs than the other complexes.

Table 4
ΔE (V) values of Fe metallic AO-PAN complexes.

Catalysts	Cu–Fe-AO-PAN(II)		Fe-AO-PAN
	Fe^{3+}/Fe^{2+}	Cu^{2+}/Cu^{+}	Fe^{3+}/Fe^{2+}
ΔE (V)	0.05	0.03	0.14

3.3. Catalytic study

3.3.1. Nature of assisted metal ions

Our previous works have found that Fe-AO-PAN can serve as an effective heterogeneous Fenton catalyst for the dye degradation in water in the dark and under visible irradiation [15,23]. In the

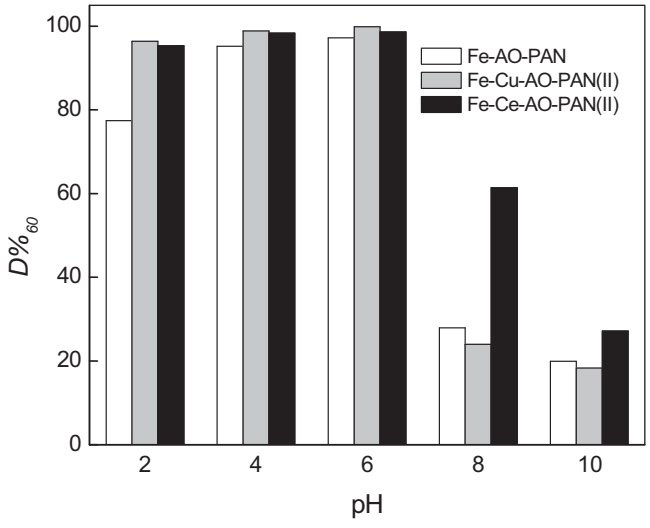

Fig. 8. RhB degradation using bimetallic AO-PAN complexes at different pH levels.

Table 5
Variation of k_d and k_r values in the presence of the catalysts with different Cu/Fe or Ce/Fe molar ratio.

Catalysts	In the dark		Under visible irradiation		$\Delta k = k_r - k_d$
	k_d (min^{-1})	R	k_r (min^{-1})	R	
Fe-AO-PAN	0.0149	0.9965	0.0492	0.9948	0.0343
Fe–Cu-AO-PAN(I)	0.0301	0.9966	0.0641	0.9973	0.0340
Fe–Cu-AO-PAN(II)	0.0502	0.9993	0.0767	0.9992	0.0265
Fe–Cu-AO-PAN(III)	0.0254	0.9980	0.0555	0.9992	0.0301
Cu-AO-PAN	0.0041	0.9907	0.0055	0.9936	0.0014
Fe–Ce-AO-PAN(I)	0.0314	0.9994	0.0778	0.9991	0.0464
Fe–Ce-AO-PAN(II)	0.0513	0.9982	0.0967	0.9957	0.0454
Fe–Ce-AO-PAN(III)	0.0254	0.9971	0.0697	0.9988	0.0443
Ce-AO-PAN	0.0045	0.9507	0.0101	0.9724	0.0056

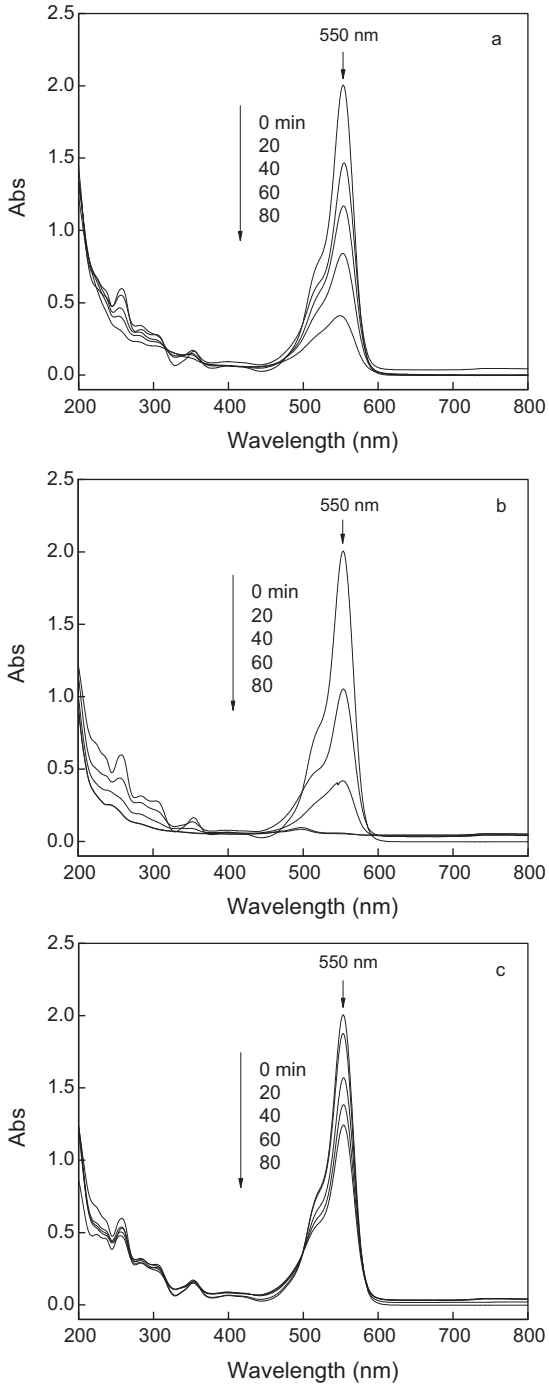

Fig. 9. Obvious changes in UV–vis spectra of RhB degradation in the three systems of (a) Fe-AO-PAN/H_2O_2, (b) Fe–Cu-AO-PAN(II)/H_2O_2 and (c) Cu-AO-PAN/H_2O_2.

present study, two transition metal ions (Cu^{2+} and Co^{2+}) and two rare earth metal ions (Ce^{3+} and La^{3+}) were used as the assisted metal ions, respectively to produce four different Fe bimetallic AO-PAN complexes with similar total metal contents and their catalytic performance was evaluated in the oxidative degradation of RhB with H_2O_2 in water. Moreover, the pseudo-first order rate constants, k_d (in the dark) and k_r (under visible irradiation) for the degradation of RhB within 40 min of reaction time were calculated with all regression coefficients greater than 0.95 and listed in Table 3.

Both k_d and k_r values in the presence of Fe bimetallic AO-PAN complexes are much higher than those in the presence of Fe-AO-PAN, indicating that Fe bimetallic AO-PAN complexes show higher catalytic activity for the dye degradation than Fe-AO-PAN at the same conditions because of the synergetic effect originated from the assisted metal ions in Fe bimetallic AO-PAN complexes. Previous studies [30,31] have reported that the enhanced catalytic activity of the bimetallic catalysts is generally ascribed to the synergistic effects in relation with high degree of interdispersion, creation of defects (e.g., oxygen vacancies) and facile redox interplay between two metals redox couples. In this work, the introduction of the assisted metal ions may significantly enhance the distortion of Fe bimetallic AO-PAN complex molecules due to the twist of PAN fiber chains [32], thus resulting in creation of defects and unsaturated coordination, which can promote the catalytic process. On the other hand, the difference between oxidative and reductive potentials (ΔE) for Cu–Fe-AO-PAN(II) and Fe-AO-PAN was measured using cyclic voltammetry method and shown in Table 4.

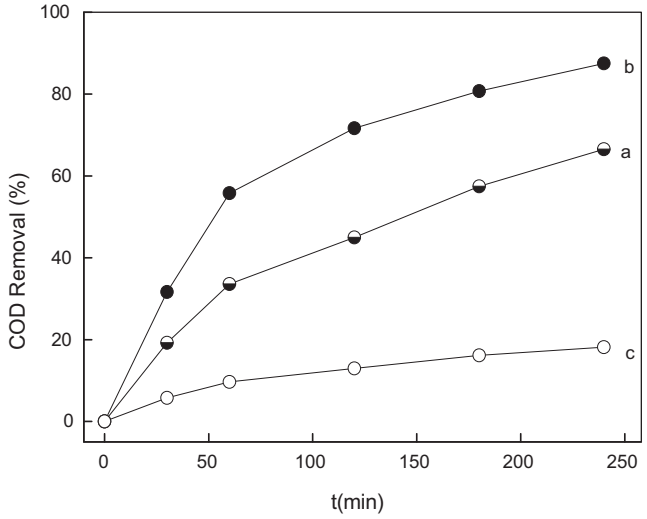

Fig. 10. Mineralization of RhB in the presence of different complexes under visible irradiation, (a) Fe-AO-PAN, (b) Fe–Cu-AO-PAN(II) and (c) Cu-AO-PAN.

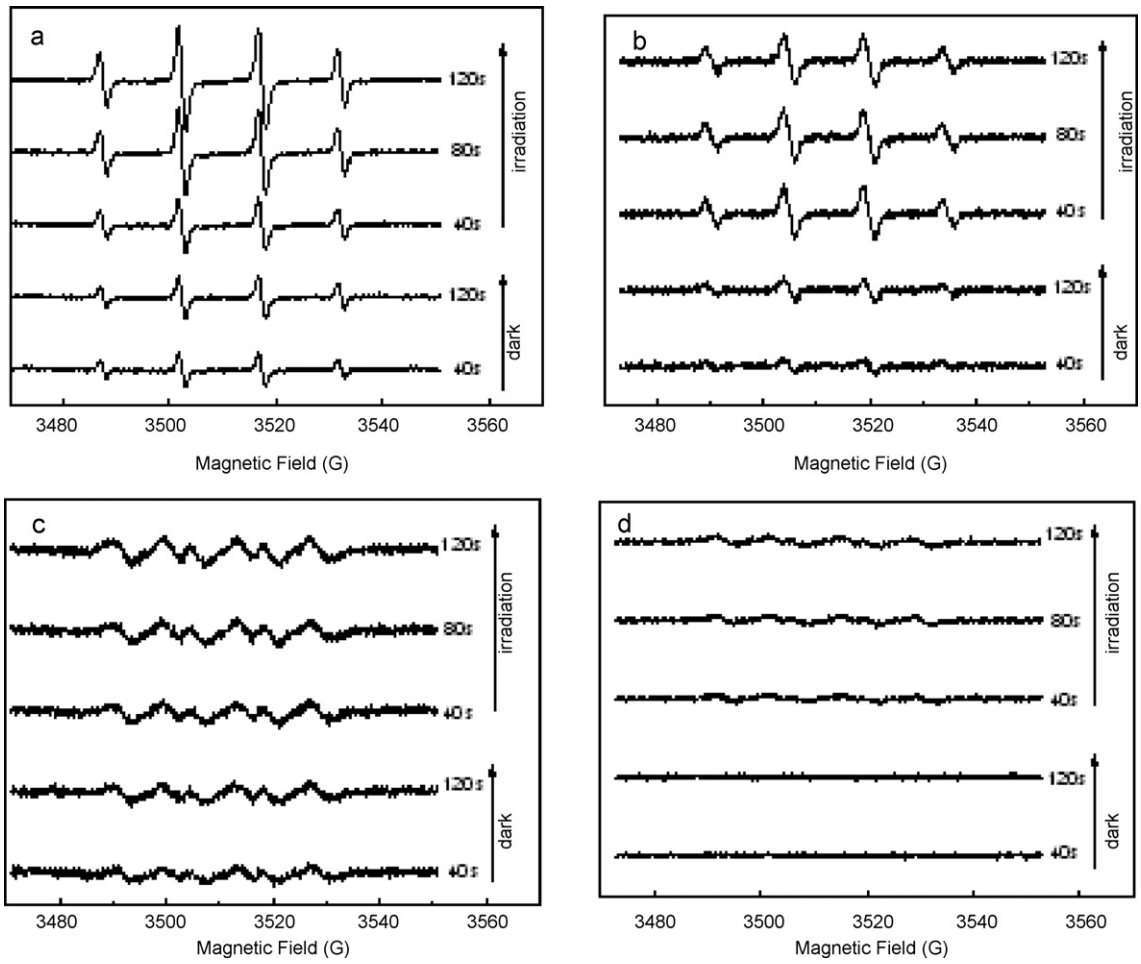

Fig. 11. DMPO spin-trapping ESR spectra recorded at ambient temperature in aqueous for DMPO-•OH (a: Fe–Cu-AO-PAN(II) and b: Fe-AO-PAN) and methanol solutions for DMPO-•OOH (c: Fe–Cu-AO-PAN(II) and d: Fe-AO-PAN) in the degradation of RhB in the presence of H_2O_2 and different catalyst.

It is clear that ΔE value for Fe^{3+}/Fe^{2+} redox of Cu–Fe-AO-PAN(II) is much lower than that of Fe-AO-PAN, suggesting that the redox potentials of Fe^{3+}/Fe^{2+} in Cu–Fe-AO-PAN(II) are more symmetric than that of Fe-AO-PAN. This may be the result of rapid transformation of Fe^{3+}/Fe^{2+} in Cu–Fe-AO-PAN(II). Moreover, Cu–Fe-AO-PAN(II) has a ΔE value for Cu^{2+}/Cu^{+} redox lower than that for Fe^{3+}/Fe^{2+} redox. This makes it possible that the redox process of Cu^{2+}/Cu^{+} ions became much easier in Cu–Fe-AO-PAN(II), thus causing a faster cycle of Cu^{2+}/Cu^{+} redox. These results indicated that an enhanced running of catalytic recycle may be obtained over Cu–Fe-AO-PAN(II), which give rise to the better catalytic ability.

It is also noticed that the visible irradiation can increase the degradation rates when these metallic AO-PAN complexes are used as the catalysts, indicating that they have the better photocatalytic performance under visible irradiation. This is due mainly to their light absorption in the visible region presented in Figs. 6 and 7. According to Lin's report [33], the initiation of H_2O_2 decomposition over iron(III) species directly relied on the formation of a photoreactive precursor surface complex such as Fe(III)–OH and Fe(III)–OOH. Fe^{3+} ions on Fe bimetallic AO-PAN complexes may react with H_2O_2 to form Fe(III)-OOH. Moreover, Fe^{3+} ions in a complex forms are readily reduced, and the obtained Fe^{2+} ions reacts with H_2O_2 to produce •OH radicals. The introduction of the light can facilitate the above reactions [34]. This reaction process is described by Eqs. (2)–(4).

$$Fe^{3+}/PAN + H_2O_2 \xrightarrow{h\nu} Fe^{3+}OOH/PAN + H^{\oplus} \quad (2)$$

$$Fe^{3+}OOH/PAN \rightarrow Fe^{2+}/PAN + HO_2\bullet \quad (3)$$

$$Fe^{2+}/PAN + H_2O_2 \rightarrow Fe^{3+}/PAN + OH_3^{\oplus} + \bullet OH \quad (4)$$

$$Dye + Fe^{3+}/PAN \xrightarrow{h\nu} Dye^{*} \cdots Fe^{3+}/PAN \rightarrow Dye^{+\bullet} + Fe^{2+}/PAN \quad (5)$$

Another possible reason is that upon visible irradiation, Fe bimetallic AO-PAN complexes are converted to exited-state transition species. Photoexcitation of the ligand-to-metal-charge-transfer (LMCT) band of Fe bimetallic AO-PAN complexes may lead to efficient intramolecular electron transfer, thus enhancing the reduction of Fe^{3+} to Fe^{2+} ion on the complexes. Additionally, it was found that the organic dye MG act as the light sensitizer of Fe^{3+} ions in the clay to lead to a conversion of Fe^{3+} to Fe^{2+} ions during photoassisted Fenton reaction [34]. In this work, we believed that RhB has the same effect as MG due to their similarity in molecular structure (Eq. (5)), which was also responsible for the higher activity of these complexes under visible irradiation. However, these Fe bimetallic AO-PAN complexes, especially two transition metal assisted Fe bimetallic complexes display the small difference between k_d and k_r than Fe-AO-PAN, implying that the presence of assisted metal ions is not favorable for the photocatalytic activity. More importantly, the rare earth metal assisted Fe bimetallic AO-PAN complexes, particularly Fe–Ce bimetallic AO-PAN complexes presented the higher k_d and k_r values for the dye degradation, especially under visible irradiation, which may be mainly associated with their unsaturated coordination environment. As mentioned above, Fe–Ce bimetallic AO-PAN complexes exhibited a more complicated coordination configuration.

Moreover, according to Pearson's hard–soft acid–base principle [17], Ce^{3+} ions coordinate preferably with the hydroxyl groups of AO-PAN to form the complexes in acidic medium, because the coordination capacity of its protonated amino groups with Ce^{3+} ions is significantly reduced, which may make it more unsaturated, thus increasing its catalytic ability. In addition, the better activity of the rare earth metal assisted Fe bimetallic AO-PAN complexes can also be associated with the improvement of redox properties of the active sites. Similar effect of the Ce addition in other heterogeneous Fenton catalysts was also observed [12].

3.3.2. Dosage of assisted metal ions

In order to investigate the impact of the assisted metal ions dosage on the catalytic performance of Fe bimetallic AO-PAN complexes, Fe–Cu or Fe–Ce bimetallic AO-PAN complexes with different Cu/Fe or Ce/Fe molar ratio were prepared with Cu^{2+} or Ce^{3+} ion as the assisted metal ion. Their Cu/Fe and Ce/Fe molar ratios were as same as those presented in Tables 1 and 2. Then these complexes were applied as the catalysts for the RhB degradation and both k_d and k_r values within 40 min of reaction time were calculated and listed in Table 5.

It is found from Table 5 that Cu-AO-PAN and Ce-AO-PAN possess much lower k_d and k_r values than Fe-AO-PAN, indicating that they have very poor ability as the Fenton catalysts. It must be pointed out that both k_d and k_r values in the presence of Fe bimetallic AO-PAN complexes are much higher than those in the presence of the monometallic AO-PAN complexes, and the maximum k_d and k_r values were achieved for Fe–Cu-AO-PAN(II) and Fe–Ce-AO-PAN(II). These results confirm that catalytic activity of Fe bimetallic AO-PAN complexes varied highly with their composition, especially Cu/Fe or Ce/Fe molar ratio, and Fe–Cu-AO-PAN(II) and Fe–Ce-AO-PAN(II) exhibit the best catalytic activity. This demonstrates that a synergetic effect between loaded Fe^{3+} and Cu^{2+} or Ce^{3+} ions in Fe bimetallic AO-PAN complexes can considerably promote their catalytic activity. Moreover, the optimum Ce/Fe molar ratio (0.174) of Fe–Ce bimetallic AO-PAN complexes was much lower than the Cu/Fe molar ratio (0.571) of Fe–Cu bimetallic AO-PAN complexes, but Fe–Ce bimetallic AO-PAN complexes show the better catalytic activity than Fe–Cu bimetallic AO-PAN complexes. Therefore, Ce^{3+} ion can be regarded as a more effective assisted metal ion for improving the catalytic activity of Fe metallic AO-PAN complexes. Additionally, Fe-AO-PAN shows a much higher Δk value than those of Cu-AO-PAN and Ce-AO-PAN, which may result from their significant difference in light absorption properties in the visible region (see Figs. 6 and 7). Comparing Δk values of two series of Fe bimetallic AO-PAN complexes, it is clear that their Δk values decrease with increasing Cu/Fe or Ce/Fe molar ratio. Fe–Cu bimetallic AO-PAN complexes with higher Cu/Fe molar ratios gave much lower Δk values. By contrast, Δk values of the Fe–Ce bimetallic AO-PAN complexes exhibit a slight reduction with increasing the Ce/Fe molar ratio, and higher than those of Fe–Cu bimetallic AO-PAN complexes. This implies that Fe–Ce bimetallic AO-PAN complexes can make a better response to visible irradiation than Fe–Cu bimetallic AO-PAN complexes. Consequently, it is believed that Fe–Ce bimetallic AO-PAN complexes are of practical importance in an industrial scale because of their unique coordination structure and strong light adsorption feature.

3.3.3. The solution pH

Fe–Cu-AO-PAN(II) and Fe–Ce-AO-PAN(II) were selected as the model photocatalysts to investigate their catalytic properties at different solution pH levels. Fig. 8 presents the decoloration percentages ($D\%_{60}$) of RhB under visible exposure with H_2O_2 catalyzed by two different bimetallic AO-PAN complexes, respectively, at a pH 2–10 range within 60 min.

Fig. 8 shows that the RhB degradation can be operated in a wide pH 2–10 range, which indicates that a significant breakdown of the dye takes place, especially at the solution pH <8. Both Fe bimetallic AO-PAN complexes have the excellent catalytic performance at acid and neutral pH medium, which is higher than the optimum pH condition for the heterogeneous photocatalysts such as Fe^{3+}/Nafion membrane [35] as well as iron oxide and silicate nanoparticles [36]. However, alkaline pH medium leads to the low $D\%_{60}$ values for two photocatalysts, especially Fe–Cu-AO-PAN(II), suggesting that they are sensitive to alkali circumstance. A possible reason is that hydroxide ions can react with metal ions loaded to form insoluble metal hydroxides that occupied part of the active sites on the catalytic surface at alkaline environment [7], which may limit the sorption of RhB on catalyst surface, thus slowing down the dye degradation rate because the sorption is a crucial step for the heterogeneous Fenton process. Another possible reason is that alkaline pH medium can significantly accelerate the H_2O_2 decomposition into O_2 and water, thus decreasing the concentration of the hydroxyl radicals generated from the heterogeneous Fenton process, which is responsible for the dye degradation. Meanwhile, it should be noticed that $D\%_{60}$ value reaches 61.4% at pH 8 in the case of Fe–Ce-AO-PAN(II), suggesting that this complex can ensure the stability as a catalyst at a wide pH range. This result has an important environmental implication from the viewpoint of low cost and energy saving, make it possible that Fenton pretreatment of the dyes is conducted without the need for adjusting subsequently the pH for further less costly biological degradation.

3.3.4. Investigation on role of Cu^{2+} as an assisted metal ion

In order to examine the effect of Cu^{2+} ion as an assisted metal ion in Fe bimetallic AO-PAN complex on the decomposition pathway of the dye molecule and the formation of aromatic intermediates during the degradation process, the photocatalytic degradation of RhB in the presence of different metallic AO-PAN complexes was examined using UV–vis spectroscopy and COD measurement and the results were shown in Figs. 9 and 10.

Fig. 9 shows that the absorbance at 200–400 nm and 400–800 nm, especially 550 nm of RhB in the presence of different complexes decrease gradually with prolonging reaction time, suggesting that the three complexes have the photocatalytic activity for not only the breaking of the conjugated chromospheres part, but also the decomposition of aromatic parts in the molecular structure. And no new peak is significantly present in the spectra during the degradation. Moreover, the decay rate of the characteristic absorbance of RhB in Fe–Cu-AO-PAN(II)/H_2O_2 system is very fast, and the final solution became colorless within 80 min. Fig. 10 shows that COD removal % of RhB in the presence of different complexes also gradually increased with the prolongation of the irradiation time. This indicates that the mineralization of RhB with H_2O_2 was effectively carried out in water when the complex was used as a photocatalyst. It is also found that COD removal efficiency of RhB by Cu-AO-PAN was very low, only reaching 18.1% after 240 min of irradiation. In both the systems where Fe-AO-PAN and Fe–Cu-AO-PAN(II) were worked as the photocatalysts, COD removal % of 66.6% and 87.5% were obtained, respectively in the same irradiation duration. The results demonstrate that Fe–Cu-AO-PAN(II) can make RhB molecules mineralize at a more rapid rate. Consequently, it is believed that Fe–Cu-AO-PAN(II) acts as a better photocatalyst with higher mineralization effectiveness for the dye mineralization than does Fe-AO-PAN. Moreover, the change in UV–vis spectra of RhB in Fe–Cu-AO-PAN(II)/H_2O_2 system is observed to be very similar to that in Fe-AO-PAN/H_2O_2 system, proposing that both Fe–Cu-AO-PAN(II) and Fe-AO-PAN complexes catalyzed the RhB oxidation with H_2O_2 through similar reaction pathway.

To further reveal the role of Cu^{2+} as an assisted metal ion in Fe metallic AO-PAN complex, spin-tripping ESR technique was used to

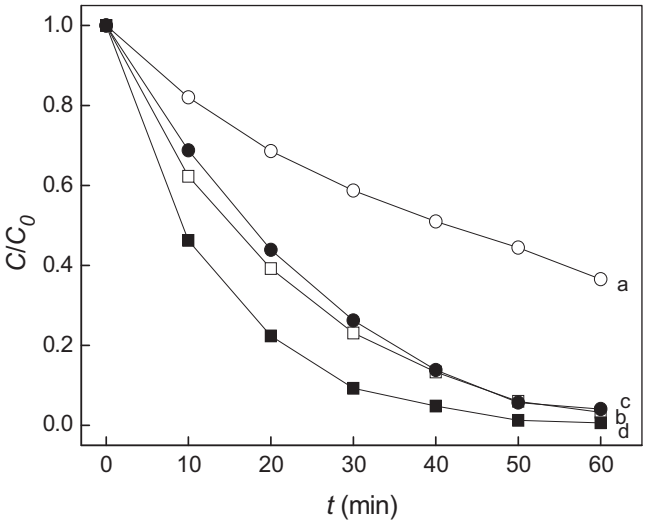

Fig. 12. H_2O_2 (3.0 mmol L^{-1}) decomposition during the RhB degradation at initial pH 6.0 and 25 °C under various conditions: (a) Fe-AO-PAN and H_2O_2 in the dark, (b) Fe–Cu-AO-PAN(II) and H_2O_2 in the dark, (c) Fe-AO-PAN and H_2O_2 under visible irradiation and (d) Fe–Cu-AO-PAN(II) and H_2O_2 under visible irradiation.

obtain information on active radicals involved (Fig. 11). When AO-PAN was used as the catalyst, no ESR signal was observed. For Fe-AO-PAN and Fe–Cu-AO-PAN(II), the characteristic peaks of DMPO-•OH adducts clearly appeared and increased with the prolongation of reaction time (Fig. 11a and b). ESR signals of •OOH radicals in two systems were also seen under visible irradiation (Fig. 11c and d). These results confirmed that both •OH and •OOH radicals have been formed in the presence of these metallic AO-PAN complexes during the reaction. It is worth noticed that Fe–Cu-AO-PAN(II) is higher than Fe-AO-PAN in terms of ESR signal intensity. On the other hand, H_2O_2 decomposition profiles during the degradation of RhB using these complexes as the catalysts were also investigated, and the results were given in Fig. 12.

Fig. 12 shows that the presence of Fe–Cu-AO-PAN(II) resulted in almost 100% decomposition of H_2O_2 within 60 min both in the dark and under visible irradiation. In the case of Fe-AO-PAN, 37% and 4% of H_2O_2 still remained, respectively within 60 min in the dark and under visible irradiation. Besides, neither the iron ions nor the copper ions were detected in the bulk solution. Furthermore, the specific surface area of Fe–Cu-AO-PAN(II) and Fe-AO-PAN were measured to be 0.619 and 0.352 $m^2\ g^{-1}$ using BET method, respectively. But, the equilibrium adsorption amounts of RhB on the two complexes were examined to be 5.0×10^{-3} mmol g^{-1} for Fe–Cu-AO-PAN(II) and 4.7×10^{-3} mmol g^{-1} for Fe-AO-PAN, respectively. This suggested that the addition of Cu^{2+} ions imposed little effect on the adsorption performance for the dye on the surface of the complex. These results have primarily proved that Cu^{2+} as an assisted metal ion in the bimetallic AO-PAN complex can promote the rapid decomposition of H_2O_2 to generate more hydroxyl radicals in the system, thus accelerating the dye degradation.

4. Conclusions

The preparation of Fe bimetallic AO-PAN complexes with different assisted metal ions was successfully accomplished. The incorporation of Cu^{2+} or Ce^{3+} ions allowed the Fe–Cu or Fe–Ce bimetallic AO-PAN complexes to have the different coordination configurations from Fe-AO-PAN complex by increasing their coordination number. The UV–vis–diffuse reflectance study shows that the Cu^{2+} or Ce^{3+} ions are present in different chemical environments in Fe bimetallic AO-PAN complexes. The light adsorption feature of Fe bimetallic AO-PAN complexes varied significantly with their Cu/Fe or Ce/Fe molar ratio. The presence of Cu^{2+} or Ce^{3+} ions caused a less intensive and blue shift adsorption of the complexes, especially Fe–Cu-AO-PAN in the visible region. The catalytic study also proved that the nature and dosage of the assisted metal ions can affect the catalytic activity of Fe bimetallic AO-PAN complexes as the catalysts for the dye degradation. Fe bimetallic AO-PAN complexes showed the better catalytic performance than Fe-AO-PAN, especially in the dark. However the addition of the assisted metal ions is not favorable for the photocatalytic activity of Fe bimetallic AO-PAN complexes. More importantly, Fe–Ce bimetallic AO-PAN complexes can lead to a more rapid decomposition of the dye with a wider pH range. On the other hand, Cu^{2+} ion is considered as a powerful assisted metal ion for Fe bimetallic AO-PAN complex catalysts because it can make the complexes better activate H_2O_2 to generate more hydroxyl radicals, subsequently oxidize dye molecules into CO_2 and water.

Acknowledgments

This work was kindly supported by a grant from the Natural Science Foundation of China (No. 20773093). The authors thank the support from the Ministry of Education of China through a grant from Research Fund for the Doctoral Program of Higher Education of China (No. 20070058005). The research was also supported in part by Key Projects in Tianjin Science and Technology Support Program from the Tianjin Municipal Committee of Science and Technology (09ZCKFSH02000).

References

[1] J. Fernandez, J. Bandara, A. Lopez, Ph. Buffat, J. Kiwi, Langmuir 15 (1999) 185–192.
[2] R. Andreozzi, A. D'Antonio, R. Marotta, Water Res. 36 (2002) 4691–4698.
[3] S.H. Bossmann, E. Oliveros, S. Gob, M. Kantor, A. Goppert, L. Lei, P.L. Yue, A.M. Braun, Water Sci. Technol 44 (2001) 257–262.
[4] J. Fernandez, J. Bandara, A. Lopez, P. Alberz, J. Kiwi, Chem. Commun. (1998) 1493–1494.
[5] J. Fernandez, M.R. Dhananjeyan, J. Kiwi, J. Phys. Chem. B 104 (2000) 5298–5301.
[6] V.V. Ishtchenko, K.D. Huddersman, R.F. Vitkovskaya, Appl. Catal. A 242 (2003) 123–137.
[7] V.V. Ishtchenko, K.D. Huddersman, R.F. Vitkovskaya, Appl. Catal. A 242 (2003) 221–231.
[8] I.R. Guimaraes, A. Giroto, L.C.A. Oliveira, M.C. Guerreiro, D.Q. Lima, J.D. Fabris, Appl. Catal. B 91 (2010) 581–586.
[9] B. Fan, H. Li, W. Fan, C. Jin, R. Li, Appl. Catal. A 340 (2008) 67–75.
[10] F. Li, X. Li, M. Hou, K. Cheah, W. Choy, Appl. Catal. A 285 (2005) 181–189.
[11] A. Prabhu, L. Kumaresan, M. Palanichamy, V. Murugesan, Appl. Catal. A 374 (2010) 11–17.
[12] Y. Zhang, X. Dou, J. Liu, M. Yang, L. Zhang, Y. Kamagata, Catal. Today 126 (2007) 387–393.
[13] J. Carriazo, E. Guélou, J. Barrault, J.M. Tatibouët, R. Molina, S. Moreno, Catal. Today 107–108 (2005) 126–132.
[14] T. Yuranova, O. Enea, E. Mielczarski, J. Mielczarski, P. Albers, J. Kiwi, Appl. Catal. B 49 (2004) 39–50.
[15] Y. Dong, Z. Han, C. Liu, F. Du, Sci. Total Environ. 408 (2010) 2245–2253.
[16] H. Bader, V. Sturzenegger, J. Hoigne, Water Res. 22 (1988) 1109–1115.
[17] G.L. Miessler, D.A. Tarr, Inorganic Chemistry, Pearson Education Asia Limited and Higher Education Press, Beijing, 2004, p. 180, 350–351.
[18] G. Henrici-Oliv, S. Oliv, Coordination and Catalysis, Verlag Chemie GmbH, Weinheim, 1977, p. 63.
[19] Y. Jeanvoine, R. Spezia, J. Phys. Chem. A 113 (2009) 7878–7887.
[20] R. Knochenmuss, E. Lehmannn, R. Zenobi, Eur. Mass Spectrom. 4 (1998) 421–427.
[21] J.E. House, Inorganic Chemistry, Elsevier Inc., 2008, pp. 685–686.
[22] J.C. Kotz, P. Treichel, Chemistry & Chemical Reactivity, fourth ed., Harcourt Brace College Publishers, 1999, pp. 1051–1052.
[23] Y. Dong, F. Du, Z. Han, Acta Phys. Chim. Sin. 24 (2008) 2114–2121.
[24] B.M. Weckhuysen, R.A. Schoonheydt, Catal. Today 49 (1999) 441–451.
[25] G.R. Rao, B.G. Mishra, Mater. Chem. Phys. 89 (2005) 110–115.
[26] H. Park, W. Choi, F.A. Cotton, G. Wilkinson, P.L. Gaus, Basic Inorganic Chemistry, John Wiley & Sons, Inc., 1995, p. 509.
[27] L. Li, J. Jin, Z. Shi, J. Liu, Y. Xing, S. Niu, Inorg. Chim. Acta 363 (2009) 748–754.
[28] H. Kunkely, A. Vogler, Inorg. Chim. Acta 358 (2005) 4086–4088.
[29] F.M.T. Mendes, M. Schmal, Appl. Catal. A 151 (1997) 393–408.
[30] J. Zhu, Q. Gao, Z. Chen, Appl. Catal. B 81 (2008) 236–243.

[31] B. Skarman, D. Grandjean, R.E. Benfield, A. Hinz, A. Andersson, L.R. Wallenberg, J. Catal. 211 (2002) 119–128.
[32] J.E. McIntyre, Synthetic Fibres, China Textile & Apparel Press, authorized by Woodhead Publishing Ltd., 2006, pp. 201–202.
[33] S. Lin, M.D. Gurol, Environ. Sci. Technol. 32 (1998) 1417–1423.
[34] M. Cheng, W. Song, W. Ma, C. Chen, J. Zhao, J. Lin, H. Zhu, Appl. Catal. B 77 (2008) 355–363.
[35] M.R. Dhananjeyan, J. Kiwi, P. Albers, O. Enea, Helv. Chem. Acta 84 (2001) 3433–3445.
[36] J. Feng, X. Hu, P.L. Yue, Ind. Eng. Chem. Res. 42 (2003) 2058–2066.